Molecular Phylogenetics and Evolution 221 (2026) 108627

Contents lists available at ScienceDirect

Molecular Phylogenetics and Evolution

journal homepage: www.elsevier.com/locate/ympev

Genome size evolution in *Helianthemum* (Cistaceae): Dynamic genomes within a conserved chromosomal framework

Sara Martín-Hernanz [a,b,*], Rafael G. Albaladejo [a], Juan Viruel [c,d], Rafael Matos [e], Sara Brito Lopes [e], Encarnación Rubio [a], Mariana Castro [e], João Loureiro [e], Polina Volkova [f], Abelardo Aparicio [a,*]

[a] Department of Plant Biology and Ecology, University of Seville, c/ Prof. García González n° 2, 4012 Seville, Spain
[b] Department of Biodiversity, Ecology and Evolution, University Complutense of Madrid, c/ José Antonio Novais n° 12, 28040 Madrid, Spain
[c] Department of Ecosystem Stewardship, Royal Kew Gardens, Kew, Richmond, Surrey TW9 3DS, UK
[d] Polytechnic School of Huesca, University of Zaragoza, Cuarte road s/n, 22071 Huesca, Spain
[e] Centre for Functional Ecology, Associate Laboratory TERRA, Department of Life Sciences, University of Coimbra, CC Martim Freitas, 3000-456 Coimbra, Portugal
[f] Papanin Institute for Biology of Inland Waters, Russian Academy of Sciences, Borok, Yaroslavl Region, 152742, Russia

ARTICLE INFO

Keywords:
Genome size
Karyotype evolution
Helianthemum
Cistaceae
Flow cytometry
Phylogenomics
Angiosperms353

ABSTRACT

Genome size is a fundamental biological characteristic, yet its evolutionary dynamics remain insufficiently understood, partly because few plant groups offer the cytogenetic and phylogenomic data required for genus-level analyses. In this study, we estimated genome size (2C values) for 80 species (c, 75% of the genus), covering all infrageneric categories (three subgenera, ten sections). Genome-size evolution was examined within a newly generated, time-calibrated phylogenetic framework based on the Angiosperms353 target-capture probe set including 89% of the species in the genus, and integrated with updated karyotype descriptors including chromosome numbers, total haploid karyotype length (THL), interchromosomal coefficient of variation in chromosome length (CV_{CL}), and intrachromosomal mean centromeric asymmetry (M_{CA}). Genome size varied 6.5-fold across the genus, ranging from 1.65 to 10.60 pg (i.e., from very small to intermediate genomes). Phylogenetically informed regressions revealed a strong positive relationship between 2C values and THL, indicating that changes in nuclear DNA content are accommodated by proportional modifications in chromosome size. In contrast, genome size showed no significant association with chromosome number or karyotype asymmetry, suggesting that genome-size diversification has occurred largely independently of major chromosomal rearrangements. Chromosome-number reconstructions confirmed a highly conserved karyotype across the genus, with only a single abrupt shift and a small number of minor dysploid changes. Ancestral-state reconstruction and comparative evolutionary modelling revealed that genome-size diversification is strongly shaped by phylogenetic structure and characterised by repeated reductions from an intermediate ancestral genome. Overall, *Helianthemum* provides a powerful model for understanding how genome size evolves within a conserved chromosomal framework.

1. Introduction

Genome size (GS) is not a random attribute of organisms and can potentially influence their evolutionary success (Veselý et al., 2020; Cacho et al., 2021). Among eukaryotes, land plants exhibit some of the most extreme values of GS variation, spanning a ~ 2,750-fold range (Pellicer et al., 2018). While whole-genome duplication (WGD, also known as polyploidization) is the most rapid and dramatic driver of genome expansion in plants, many lineages exhibit massive GS variation without changes in ploidy level (Vitales et al., 2020; Moraes et al., 2022). GS dynamics not related to WGD across both diploid and polyploid lineages are fundamentally driven by the accumulation and removal of non-coding repetitive DNA, diverse classes of transposable elements (e.g., LTR-retrotransposons) and tandem repeats (e.g., satellite

* Corresponding authors at: Department of Biodiversity, Ecology and Evolution, University Complutense of Madrid, Madrid, Spain (S. Martín-Hernanz) and Department of Plant Biology and Ecology, University of Seville, Spain (A. Aparicio).
E-mail addresses: sarmar37@ucm.es (S. Martín-Hernanz), abelardo@us.es (A. Aparicio).

https://doi.org/10.1016/j.ympev.2026.108627
Received 2 December 2025; Received in revised form 10 April 2026; Accepted 18 April 2026
Available online 19 April 2026

DNA), as well as by chromosomal rearrangements. These rearrangements can be broadly categorized into those that modify genome structure without altering the chromosome count—such as inversions, reciprocal translocations, and massive segmental deletions or duplications—and those that generate dysploid changes in chromosome number, primarily through chromosome fusions and fissions (Moraes et al., 2022; Schubert and Lysák, 2011). Together, these mechanisms highlight that GS is highly dynamic: while the proliferation of repetitive elements can lead to substantial genome expansion, excessive increases may become counterbalanced by continuous genome-downsizing processes (Leitch and Bennett, 2004; Bennetzen et al., 2005).

Crucially, these DNA content fluctuations and structural rearrangements leave measurable karyotypic signatures, including variation in total haploid karyotype length (THL) and intra- or interchromosomal asymmetry (Weiss-Schneeweiss and Schneeweiss, 2013; Du et al., 2017). To unravel how GS evolves and interacts with these chromosomal changes, densely sampled studies at the genus level offer particularly strong analytical power (Hawkins et al., 2008). However, comprehensive analyses jointly examining GS and detailed karyotype descriptors within a robust phylogenetic framework remain rare (e.g., Carta and Peruzzi, 2015; Wang et al., 2023; Weiss-Schneeweiss et al., 2006). Integrating both datasets is essential to clarify whether changes in DNA content are strictly coupled with structural chromosomal reorganizations or proceed independently during plant diversification.

The Palearctic genus *Helianthemum* (L.) Mill. (Cistaceae Juss.) represents an excellent model for studying genome size evolution. This monophyletic lineage comprises about 107 species currently classified into three subgenera (including the recently described subg. *Eriocarpum* (Dunal) Martín-Hernanz, Velayos, Albaladejo & Aparicio) and ten sections (Martín-Hernanz et al., 2021a). *Helianthemum* is primarily distributed across the Mediterranean Basin, but also extending into Macaronesia, Central and Northern Europe, North Africa, and Central Asia (Aparicio et al., 2017; Martín-Hernanz et al., 2021b). Driven by a rapid and recent diversification since the Late Miocene—which comprises three major evolutionary radiations corresponding to the largest taxonomic sections of each subgenus (Martín-Hernanz et al., 2019)—its species have colonized a wide variety of environments, ranging from alpine meadows to semideserts, steppes, and oceanic islands.

Concomitant with this ecological diversification, *Helianthemum* exhibits pronounced life-history and morphological heterogeneity. Growth forms range from ephemeral annuals (therophytes) to woody perennial chamaephytes and subshrubs. Furthermore, the genus displays a broad spectrum of reproductive strategies, encompassing three distinct floral morphologies linked to varying breeding systems (Martín-Hernanz et al., 2023a). Crucially, despite this extensive ecological and phenotypic radiation, the genus retains a highly conserved chromosome number (mostly $2n = 20, 22$) and stable karyotype symmetry (Martín-Hernanz et al., 2023b). However, it exhibits substantial variation in total haploid karyotype length (THL) across closely related species (Martín-Hernanz et al., 2023b). This decoupling of traits provides a unique opportunity to study GS evolution independently of polyploidy or major chromosomal restructuring, which are the typical drivers of genomic variation in most other plant groups (e.g., Bennetzen et al., 2005; Pellicer et al., 2018).

Here, we investigate GS variation (2C values) and its evolution using a newly generated, densely sampled, time-calibrated phylogenetic framework based on the Angiosperms353 universal target-capture probe set (Johnson et al., 2019) including 95 *Helianthemum* species (c. 89% of the genus). We integrate these GS estimates with an expanded set of karyotype descriptors derived from recent cytogenetic work (Martín-Hernanz et al., 2023b), including chromosome numbers, THL, interchromosomal coefficient of variation in chromosome length (CV_{CL}), and intrachromosomal mean centromeric asymmetry (M_{CA}). Our overarching goal is to explore how GS covaries with chromosomal structure and to understand the macroevolutionary dynamics of GS across the genus. Specifically, we address four central aims: (i) quantify the extent and taxonomic distribution of GS variation within *Helianthemum,* (ii) characterise the mode of GS evolution along a robust time-calibrated phylogeny, (iii) test the relationships between GS and key karyotype descriptors (chromosome number, THL, and asymmetry indices); and (iv) reassess chromosome-number evolution using the updated phylogeny and cytogenetic dataset to determine the patterns and rates of dysploid change in the genus. Based on general principles of plant genome evolution (Garnatje et al., 2004; Vitales et al., 2020; Du et al., 2017; Senderowicz et al., 2021; Zhang et al., 2025) and previous work in *Helianthemum* (Martín-Hernanz et al., 2023b), we expect GS to correlate strongly with THL, but to remain largely independent of chromosome number and karyotype asymmetry, given the rarity of dysploidy and structural rearrangements in the genus. Furthermore, considering that *Helianthemum* has undergone three recent and rapid evolutionary radiations, we hypothesize that the extensive variation in GS did not accumulate through a strictly gradual process, but rather followed a more complex or episodic mode of evolution.

2. Material and methods

2.1. Taxon sampling

To investigate genome size evolution and establish a robust phylogenetic framework for *Helianthemum*, we carried out a comprehensive sampling covering all major infrageneric lineages (three subgenera, ten sections) across the entire geographic and ecological range of the genus. Following the recent descriptions of narrow endemics (e.g., *H. henriquezii* A.Rebolé, A.Acevedo & A.García, *H. tibiabinae* Marrero-Rodr., Díaz-Bertrana & S.Scholz, and *H. bilyanense* Serra, J.C.Hern., M.Á.Alonso & M.B.Crespo; Rebolé et al., 2021; Marrero-Rodríguez et al., 2023; Serra et al., 2023), we currently recognize 107 species in the genus (Martín-Hernanz et al., 2021a). Because of the different methodological requirements for flow cytometry and phylogenomic analyses, our sampling was divided into two highly overlapping datasets.

Regarding the phylogenomic dataset, our sampling for the Angiosperms353 target-capture sequencing (Johnson et al., 2019) expands previous phylogenetic reconstructions based on Genotyping-by-sequencing (GBS; Martín-Hernanz et al., 2019) by incorporating taxa from previously unsampled regions, including the Horn of Africa, southern Arabia, and the Caucasus. We sampled 181 individuals representing 124 ingroup taxa (95 species and 34 subspecies) alongside two outgroups (*Cistus ladanifer* L. and *C. lasianthus* Lam.). This yields a species-level coverage of 88.8% of the currently recognized species in the genus, covering all three subgenera and ten sections (Table S1). Leaf material for this dataset was obtained from field collections and selected herbarium specimens.

For the genome size and karyotypic dataset, we sampled a total of 83 *Helianthemum* taxa (representing 80 species and 10 subspecies), which corresponds to a species-level coverage of 74.8% of the genus. Genome size was estimated from 2C values obtained by flow cytometry (Doležel et al., 2007) using seeds collected from natural populations during field expeditions or sourced from seed banks (Fig. 1; Table S2). Furthermore, this seed sampling builds on previous karyological work (Martín-Hernanz et al., 2023b) to extract an expanded set of karyotype descriptors, including four newly added taxa: *H. citrinum* subsp. *kachchicum* Patel RM, Prajapati RS and Gosavi KVC (Patel et al., unpublished), *H. guerrae* Sánchez-Gómez, J.S.Carrion and M.A.Carrión, *H. obtusifolium* Dunal, and *H. polygonoides* Peinado, Mart.Parras, Alcaraz and Espuelas. In total, the expanded cytogenetic dataset comprises 96 source populations. Finally, voucher specimens for all newly collected materials have been deposited in the herbarium of the University of Seville (SEV).

2.2. Phylogenetic framework based on Angiosperms353 target-capture probe set

Total genomic DNA was extracted using a modified CTAB protocol

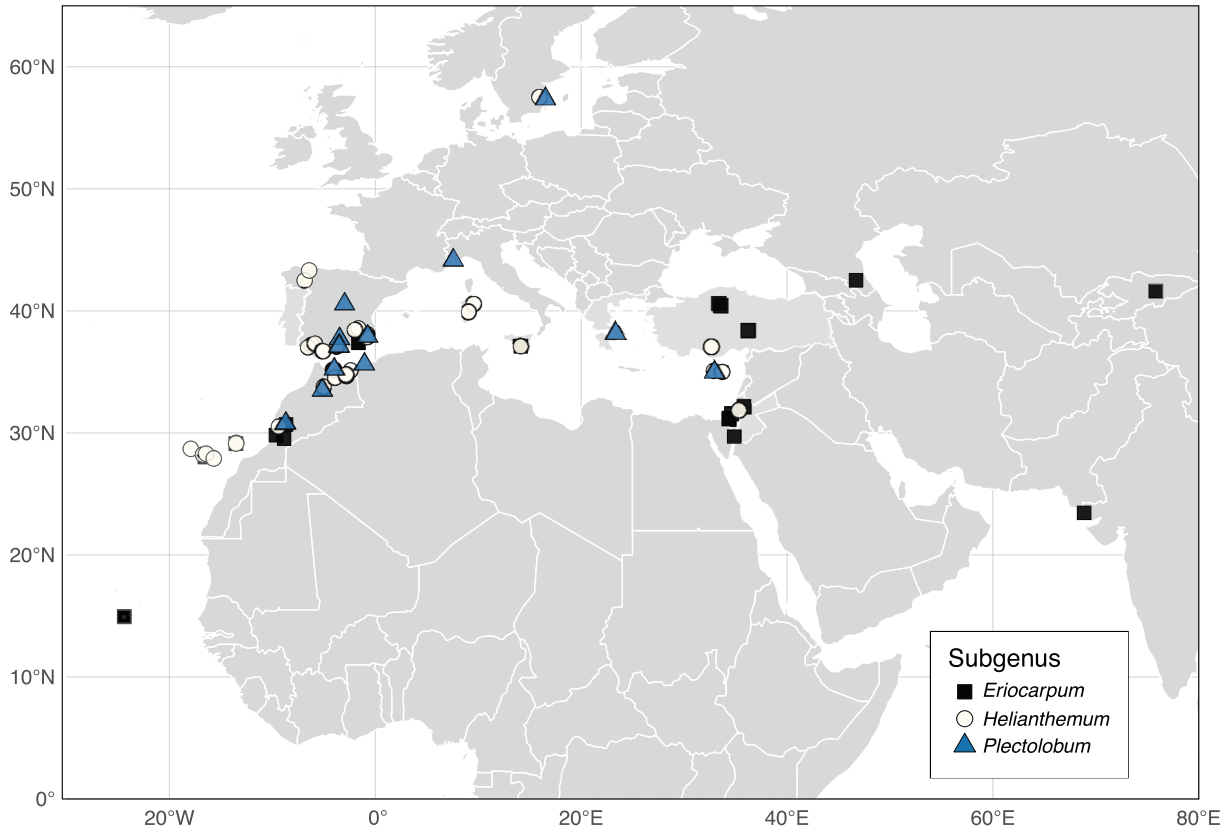

Fig. 1. Locations of the *Helianthemum* source populations from which the seeds used for karyotyping and genome-size estimation were collected.

(Doyle and Doyle, 1987). Genomic libraries were prepared with the NEBNext Ultra II DNA Library Prep Kit, enriched with the Angiosperms353 probe set following the myBaits protocol at half volume (Arbor Biosciences), and sequenced as 2 × 150 bp paired-end reads on an Illumina HiSeq platform. Full laboratory and bioinformatic details are provided in Methods S1.

Raw reads were quality-filtered with Trimmomatic v.0.36 (Bolger, Lohse and Usadel, 2014) and assembled using HybPiper v.2.0 (Johnson et al., 2016) to recover coding regions and flanking introns for the 353 target genes. Genes flagged for paralogy or represented in fewer than 30% of samples were discarded. The remaining supercontigs were aligned with MAFFT v.7.505 using the –-auto option (Katoh et al., 2002), trimmed with trimAl v.1.4.1 (Capella-Gutiérrez et al., 2009), and concatenated into a single matrix with FASconCAT v.1.11 (Kück and Meusemann, 2010). The final dataset comprised 194 loci and 181 samples.

Phylogenetic inference was performed using both concatenation and coalescent approaches. Maximum Likelihood (ML) analyses of the concatenated matrix were conducted in IQ-TREE v.2.2.2.6 (Minh et al., 2020) under a General Time-Reversible model with Gamma-distributed rate heterogeneity (GTR + G) substitution model with 1000 ultrafast bootstrap replicates (Hoang et al., 2018). Coalescent analyses were run by estimating a ML tree for each locus under the same model and summarising them with ASTRAL-III v.5.7.8 (Zhang et al., 2018). Because both approaches yielded highly congruent topologies and the concatenated analysis provided greater resolution at shallow nodes, the concatenated tree was used for divergence-time estimation.

Prior to divergence time estimation, the majority-rule consensus tree and the 1000 bootstrap trees from the IQ-TREE analysis were pruned to retain a single representative per species, using drop.tip() in *ape* (Paradis and Schliep, 2019). Divergence times were then estimated on these pruned trees using a penalised-likelihood approach in TreePL v.1.0 (Smith and O'Meara, 2012), applying four secondary calibrations from Martín-Hernanz et al. (2019), including the crown node of *Helianthemum* and the crown nodes of the three largest sections. The optimal smoothing parameter was selected via random subsample and replicate cross-validation. To incorporate phylogenetic uncertainty, the majority-rule consensus tree and 1000 bootstrap trees from the IQ-TREE analysis were dated independently and summarised with TreeAnnotator v.1.8.4 (Drummond and Rambaut, 2007).

Once the time-calibrated phylogeny was established, a subsequent and independent pruning step was required to study the evolution of genome size and chromosome number, and to evaluate the relationship between genome size and karyotype descriptors. Specifically, the fully dated tree was pruned to strictly retain the overlapping subset of 82 taxa for which complete empirical data on both genome size and chromosomal variables were available. Excluding taxa with missing trait data is a standard requirement in phylogenetic comparative methods to prevent algorithms from interpolating unknown ancestral states, which could introduce analytical artefacts (Moeglein et al., 2020; Elliott et al., 2022). All raw reads, alignments, supercontig matrices, calibration priors and resulting phylogenies are deposited in Zenodo (https://doi.org/10.5281/zenodo.17050311) and National Center for Biotechnology Information Sequence Read Archive (NCBI SRA) under BioProject PRJNA1219060.

2.3. Genome size estimation

GS was estimated from 2C values obtained by flow cytometry (Doležel et al., 2007). Genome size was calculated from fluorescence ratios between the sample and the internal standard. In most instances, GS estimates were obtained from the same seed pool used for cytogenetic analyses, allowing integration of nuclear DNA content with karyotype descriptors at population level.

For each sample, nuclei were isolated from 2 to 5 intact seeds (without any prior pre-treatment or germination). Given the very small

size of *Helianthemum* seeds (c. 1 mm in length), pooling this quantity was required to ensure an adequate nuclei yield. The seeds were co-chopped with 50 mg of leaf tissue from an internal reference standard selected according to the expected 2C value (pg DNA) of the target species: *Raphanus sativus* L. (2C = 1.11), *Solanum lycopersicum* L. (2C = 1.96), *Bellis perennis* L. (2C = 3.70), or *Pisum sativum* L. (2C = 9.09). Nuclei were extracted in Woody Plant Buffer (WPB; Loureiro et al., 2007) and stained with propidium iodide.

Filtered nuclei suspensions (50 μm nylon mesh) were incubated for 5 min at room temperature with 50 μg/mL propidium iodide (Fluka, Buchs, Switzerland). Fluorescence was measured using a Sysmex CyFlow Space flow cytometer (532 nm green solid-state laser, 30 mW; Partec GmbH, Görlitz, Germany). Data were processed with Partec FloMax v2.4d (Partec GmbH, Münster, Germany), generating four histograms per sample: (1) fluorescence pulse integral (FL) in linear scale, (2) forward scatter (FS) vs. side scatter (SS) in logarithmic scale, (3) FL vs. time, and (4) FL vs. SS in log scale. A polygonal gate was applied to FL vs. SS plots to exclude debris (Fig. S1).

Holoploid genome size (2C) was calculated following Doležel et al. (2007) using the formula:

$$\text{Holoploid genome size (GS)} = \frac{\textit{Helianthemum}\ \text{G1 peak mean}}{\text{internal standard G1 peak mean}} \times \text{internal standard GS}$$

Finally, GS values were categorized following Leitch et al. (1998) into: very small ($2C \leq 2.8$ pg), small (2.8 pg $< 2C \leq 7.0$ pg), and intermediate (7.0 pg $< 2C \leq 28.0$ pg).

2.4. Karyotype descriptors

Following the methodology detailed in Martín-Hernanz et al. (2023b), karyotype parameters for the newly added taxa were obtained from high-quality mitotic metaphase spreads using MATO (Measurement and Analysis Tools; Altinordu et al., 2016). To ensure consistency across the expanded dataset, summary statistics at the genus, subgenus, and section levels are here recalculated to incorporate the newly added taxa (Table 1). The dataset includes five key karyotype descriptors that capture both chromosome size and symmetry: (1) total haploid (monoploid) karyotype length (THL; Altinordu et al., 2016); (2) karyotype formula (Levan et al., 1964); (3) karyotype asymmetry class sensu Stebbins (1971); (4) interchromosomal coefficient of variation in chromosome length (CV_{CL}; Paszko, 2006); and (5) intrachromosomal mean centromeric asymmetry (M_{CA}; Peruzzi and Eroğlu, 2013).

2.5. Genome size evolution

Phylogenetic signal in genome size was quantified using Blomberg's K (Blomberg et al., 2003) and Pagel's λ (Pagel, 1999), both implemented in phylosig() in *phytools* (Revell, 2012). Blomberg's K evaluates the degree to which closely related species resemble each other relative to Brownian expectations, whereas λ assesses the extent to which trait covariance matches the structure and branch lengths of the phylogeny. To characterise the tempo and mode of genome size evolution, we fitted alternative continuous-trait evolutionary models using ML as implemented in fitContinuous() in *geiger* v2.0 (Harmon et al., 2008; Pennell et al., 2014). Analyses were performed on log-transformed genome size values and used an ultrametric version of the dated phylogeny to ensure comparability among models. We evaluated four standard models: a Brownian Motion model (BM), an Ornstein–Uhlenbeck model with a single selective optimum (OU), an Early-Burst model (EB) describing an exponential decline in evolutionary rates through time, and a White-noise model (WN) lacking phylogenetic structure. Model support was assessed using Akaike Information Criterion corrected (AICc) for small samples.

To investigate the evolutionary dynamics of GS, we reconstructed ancestral GS values across the time-calibrated phylogeny using the function contMap() in *phytools*. Genome size was treated as a continuous trait, and both tip and internal nodes were colour-coded according to haploid chromosome number (n). Details on how chromosome numbers were inferred along the phylogeny are provided in the following section ("Updating chromosome number evolution"). The ancestral GS reconstruction was visualised using a fan-shaped phylogram, with genus-standardised taxon names assigned to the tips for clarity.

2.6. Correlation with karyotype descriptors

To examine the correlates of GS with karyotypic descriptors, we assessed phylogenetically informed associations using Phylogenetic generalized least squares (PGLS) models implemented with the *phylolm v.2.6.5* package (Ho and Ané, 2014), with chromosome number, THL, CV_{CL} and M_{CA} as predictor variables. To account for uncertainty in parameter estimates, we generated confidence intervals for the predicted values using a nonparametric bootstrap procedure. Specifically, 1000 bootstrap replicates were created by resampling the residuals of the fitted PGLS model with replacement, and for each replicate, the predicted values were recalculated. The 95% confidence intervals were then derived from the 2.5th and 97.5th percentiles of the bootstrap distribution.

2.7. Updating chromosome number evolution

Chromosome number evolution in *Helianthemum* has previously been reconstructed using phylogenies based on Sanger sequences (Aparicio et al., 2019) and GBS data (Martín-Hernanz et al., 2019). Here, we update these analyses by incorporating four newly generated chromosome counts and by using the new time-calibrated phylogeny derived from Angiosperms353 target-capture data. The phylogeny was pruned to retain a single representative per taxon, resulting in a final dataset of 80 tips. *Helianthemum ordosicum* Y.Z. Zhao, Zong Y. Zhu and R. Cao (reported as 2n = 4x = 40) was excluded pending confirmation of its polyploid status as well as casual tetraploid populations of *H. ledifolium* (L.) Miller and *H. aegyptiacum* (L.) Miller (Rice et al., 2015) [see Martín-Hernanz et al. (2023b) for a discussion].

It is also novel in this study that chromosome number evolution has been inferred using the ML framework implemented in ChromEvol v3.0 (Shafir et al., 2024). This new version allows for the detection of heterogeneous rates across the phylogeny, accounting for clades that may exhibit distinct patterns of chromosome-number change. Following previous reconstructions (Aparicio et al., 2019; Martín-Hernanz et al., 2023b), which consistently identified the CONSTANT-RATE MODEL without duplication as the best fit and considering the general stability of chromosome numbers in *Helianthemum* (n = 10, 11, 12), we set both gain (λ) and loss (ρ) rates to be constant (CONST) across the entire phylogeny. Polyploidy and demiploidy events were excluded by setting their rates to IGNORE, and the ancestral chromosome number at the root was fixed at n = 10. To test the hypothesis of localized rate shifts, particularly in the branch leading to the unique n = 5 species [*H. squamatum* (L.) Dum.Cours.], we ran a HETEROGENEOUS model allowing for the detection of rate accelerations in small clades or single branches (minCladeSize parameter set to 1). We compared the best HETEROGENEOUS models against the null (HOMOGENEOUS) model using AICc, considering models with ΔAICc < 2 as significantly better supported.

3. Results

3.1. Phylogenetic framework based on Angiosperms353 target-capture data

We successfully recovered nuclear target capture data for 181 samples of *Helianthemum*, plus *Cistus ladanifer* and *C. lasianthus* as outgroups

Table 1
Cytogenetic data surveyed in this study across subgenus, section, and species level within the genus *Helianthemum*. n =, inferred haploid chromosome number. ID, number of the source population; 2C, Mean 2C-values (pg DNA) ± SE (Greilhuber et al., 2005). N, number of metaphase spreads analysed. THL, mean total monoploid length (μm) of chromosome set (Altinordu et al., 2016). CV, coefficient of variation of mean THL. Karyotype formula (Levan et al., 1964) and the karyotype asymmetry classification of Stebbins (Stebbins, 1971). CV_{CL}, coefficient of variation of chromosome length (Paszko, 2006). M_{CA}, mean centromeric asymmetry (Peruzzi & Eroğlu, 2013). Nomenclature follows Martín-Hernanz et al. (2021b). All values were computed using MATO (Altinordu et al., 2016). Asterisks after a scientific name indicate taxa added in this study compared to Martín-Hernanz et al. (2023a).

	n =	ID	2C	N	THL	CV	Karyotype formula	Stebbins' Karyotype asymmetry	CV_{CL} ± SE	M_{CA} ± SE
GEN. *HELIANTHEMUM* Mill.	**5, 10, 11, 12**		**5.18 ± 0.22**	**743**	**31.62**	**26.84**			**15.38 ± 0.37**	**22.47 ± 0.43**
SUBG. *ERIOCARPUM* (Dunal) Martín-Hernanz, Velayos, Albaladejo & Aparicio	**5, 10, 11**		**2.93 ± 0.38**	**188**	**22.39**	**27.26**			**16.73 ± 0.78**	**20.71 ± 0.97**
SECT. *ARGYROLEPIS* Spach	**5**		**5.96**	**9**	**24.57**	–			**14.52**	**10.91**
H. squamatum (L.) Dum.Cours.	5	239	5.96	9	24.57	7.13	10 *m*	1A	14.52 ± 1.80	10.91 ± 0.73
SECT. *LAVANDULACEUM* G.López	**10**		**7.15 ± 0.04**	**19**	**37.27**	**3.07**			**14.11 ± 1.36**	**28.06 ± 5.26**
H. motae Sánchez-Gómez, Jiménez & Vera	10	277	7.18	8	36.46	9.61	4 m + 16sm	3A	15.47 ± 0.80	33.32 ± 0.59
H. syriacum (Jacq.) Dum.Cours.	10	17	7.11	11	38.08	9.65	14 m + 6sm	2A	12.76 ± 0.97	22.81 ± 0.56
SECT. *ERIOCARPUM* Dunal	**10**		**1.99 ± 0.05**	**109**	**18.93**	**6.58**			**18.09 ± 1.00**	**19.28 ± 0.34**
H. canariense (Jacq.) Pers.	10	402, 403	1.95	7	17.68	9.21	16 m + 4sm	1A	17.51 ± 1.13	18.80 ± 1.30
H. citrinum subsp. *kachchicum* Patel RM, Prajapati RS and Gosavi KVC. *	10	663	2.15	5	18.91	5.28	16 m + 4sm	1A	16.48 ± 0.99	19.09 ± 1.37
H. confertum Dunal	10	525	2.02	10	19.33	9.33	17 m + 3sm	1A	20.19 ± 1.32	20.18 ± 1.05
H. ellipticum (Desf.) Pers.	10	374	2.03	10	19.19	8.06	16 m + 4sm	2A	21.04 ± 1.46	20.79 ± 2.39
H. gorgoneum Webb	10	348, 349, 351	2.10	9	18.66	8.99	20 *m*	1A	17.16 ± 1.04	17.35 ± 0.96
H. kahiricum Delile	10	374	2.11	8	19.71	7.63	19 m + 1sm	1A	22.35 ± 1.30	18.32 ± 0.69
H. lippii (L.) Dum.Cours	10	283	1.68	6	17.52	6.91	16 m + 4sm	2A	22.47 ± 1.61	19.09 ± 1.06
H. sancti-antonii Schweinf.	10	642	2.15	9	20.59	7.42	20 *m*	1A	16.52 ± 0.97	18.98 ± 1.05
H. sessiliflorum (Desf.) Pers.	10	384, 385	1.65	13	16.91	9.35	16 m + 4sm	1A	17.65 ± 0.93	18.38 ± 1.39
H. sicanorum Brullo, Giusso & Sciandr.	10	297	2.18	8	21.21	5.11	20 *m*	1A	20.15 ± 0.93	20.38 ± 0.88
H. stipulatum (Forssk.) C.Chr.	10	290, 382	1.82	6	18.69	4.49	17 m + 3sm	1A	20.58 ± 1.11	20.13 ± 0.37
H. thymiphyllum Svent.	10	409, 410	1.94	6	18.17	9.33	18 m + 2sm	1A	15.92 ± 1.14	19.99 ± 0.93
H. ventosum Boiss.	10	644	2.07	12	19.04	9.07	18 m + 2sm	1A	14.82 ± 1.12	20.18 ± 1.15
SECT. *PSEUDOMACULARIA* Grosser	**11**		**3.11 ± 0.26**	**51**	**25.67**	**14.66**			**14.17 ± 0.64**	**24.11 ± 0.64**
H. antitauricum Davis & Coode	11	647	2.89	10	27.86	9.04	10 m + 12sm	2A	15.79 ± 0.99	25.91 ± 1.13
H. dagestanicum Rupr.	11	448	2.60	13	20.65	9.15	14 m + 8sm	1A	14.27 ± 0.49	24.12 ± 0.62
H. germanicopolitanum Bornm.	11	645, 648	3.13	14	24.57	4.80	13 m + 9sm	2A	12.65 ± 0.53	23.78 ± 0.75
H. songaricum Zhao, Zhu & Cao	11	643	3.82	14	29.12	6.59	15 m + 7sm	2A	13.97 ± 0.47	23.02 ± 0.85
SUBG. *PLECTOLOBUM* Willk.	**11, 12**		**5.84 ± 0.35**	**137**	**38.27**	**16.78**			**14.30 ± 0.50**	**20.23 ± 1.04**
SECT. *CAPUT-FELIS* G.López	**12**		**6.58**	**9**	**44.03**	–			**15.27**	**13.66**
H. caput-felis Boiss.	12	275	6.58	9	44.03	5.93	24 *m*	1A	15.27 ± 0.53	13.66 ± 0.55
SECT. *ATLANTHEMUM* (Raynaud) G. López, Ortega Oliv. & Romero García	**11**		**3.06**	**6**	**24.09**	–			**18.70**	**26.04**
H. sanguineum (Lag.) Lag. ex Dunal in DC.	11	295	3.06	6	24.09	6.83	13 m + 9sm	2A	18.70 ± 1.22	26.04 ± 1.42
SECT. *MACULARIA* Dunal	**11**		**4.89 ± 1.67**	**14**	**30.82**	**39.20**			**12.69 ± 1.38**	**25.24 ± 5.44**
H. lunulatum (All.) DC.	11	500	6.55	6	39.37	7.37	14 m + 8sm	2A	14.07 ± 0.81	19.80 ± 0.70
H. pomeridianum Dunal	11	352	3.22	8	22.27	9.89	5 m + 17sm	2A	11.32 ± 0.97	30.68 ± 2.47

(*continued on next page*)

Table 1 (*continued*)

	n =	ID	2C	N	THL	CV	Karyotype formula	Stebbins' Karyotype asymmetry	CV_{CL} ± SE	M_{CA} ± SE
SECT. *PSEUDOCISTUS* Dunal	**11**		**6.77 ± 0.17**	**108**	**40.39**	**4.76**			**14.11 ± 0.46**	**19.39 ± 1.06**
H. cinereum subsp. *rotundifolium* (Dunal) Greuter	11	429	6.18	12	37.14	8.88	17 m + 5sm	2A	13.53 ± 0.48	19.46 ± 0.74
H. frigidulum Cuatrecasas	11	619	6.57	10	38.61	9.91	19 m + 3sm	2A	15.53 ± 0.21	18.43 ± 0.59
H. hymettium Boiss. & Heldr.	11	534	7.20	10	41.48	6.85	14 m + 8sm	2A	15.81 ± 0.54	20.38 ± 0.71
H. origanifolium subsp. *africanum* B.Crespo, M.A. Alonso, A.Vicente & J.L.Villar	11	621	6.50	7	41.98	6.42	18 m + 4sm	2A	13.73 ± 1.13	18.50 ± 0.72
H. marifolium subsp. *andalusicum* (Font Quer & Rothm.) G.López	11	49	6.42	14	42.16	8.85	14 m + 8sm	2A	15.14 ± 0.40	21.06 ± 0.43
H. oelandicum (L.) DC: subsp. *oelandicum*	11	576	6.17	7	39.31	9.98	15 m + 7sm	2A	12.36 ± 1.25	18.28 ± 0.90
H. oelandicum subsp. *conquense* (Borja & Rivas Goday ex G.López) Martín-Hernanz, Velayos, Albaladejo & Aparicio	11	242	6.72	10	39.14	9.71	17 m + 5sm	2A	15.59 ± 0.54	20.89 ± 0.61
H. pannosum Boiss.	11	615	6.72	6	40.77	4.52	14 m + 8sm	2A	14.63 ± 0.36	23.45 ± 0.86
H. polyanthum (Desf.) Pers.	11	117	8.08	12	43.80	8.64	12 m + 10sm	2A	16.07 ± 0.55	23.23 ± 0.66
H. raynaudii Ortega Oliv., Romero García & C. Morales	11	70	6.68	8	39.35	4.86	16 m + 6sm	2A	13.50 ± 0.91	16.63 ± 0.74
H. viscidulum Boiss.	11	81	7.22	11	40.67	7.11	16 m + 6sm	2A	11.61 ± 0.38	18.33 ± 0.44
SUBG. *HELIANTHEMUM*	**10**		**5.79 ± 0.22**	**418**	**33.42**	**19.87**			**15.14 ± 0.52**	**23.93 ± 0.43**
SECT. *BRACHYPETALUM* Dunal	**10**		**3.14 ± 0.06**	**24**	**21.70**	**5.13**			**21.73 ± 0.89**	**24.74 ± 0.81**
H. angustatum Pomel	**10**	82	3.24	5	21.94	8.06	12 m + 8sm	2A	23.60 ± 0.97	26.08 ± 1.35
H. ledifolium (L.) Mill.	10	423	3.00	5	22.83	3.97	14 m + 6sm	2A	22.04 ± 1.63	22.38 ± 1.00
H. papillare Boiss.	10	262	3.07	7	21.86	9.09	12 m + 8sm	2A	19.30 ± 1.16	25.12 ± 0.71
H. salicifolium (L.) Mill.	10	288, 290, 297	3.23	7	20.16	5.74	12 m + 8sm	2A	22.03 ± 0.83	25.38 ± 1.69
SECT. *HELIANTHEMUM*	**10**		**6.03 ± 0.21**	**394**	**34.50**	**16.91**			**14.53 ± 0.44**	**23.85 ± 0.45**
H. aegyptiacum (L.) Mill.	10	123	4.06	11	27.23	6.16	6 m + 14sm	3A	13.43 ± 0.55	23.23 ± 0.72
H. aganae Marrero Rodr. & R.Mesa	10	435	5.21	8	26.34	8.98	12 m + 8sm	2A	14.52 ± 0.54	10.91 ± 0.92
H. aguloi Marrero Rodr. & R.Mesa	10	436	4.79	10	27.78	9.90	16 m + 4sm	1A	11.44 ± 0.67	21.60 ± 0.89
H. almeriense Pau	10	47	6.25	8	39.55	8.296	9 m + 11sm	2A	15.49 ± 0.79	24.23 ± 1.05
H. alypoides Losa & Rivas Goday	10	45	6.51	8	37.47	9.22	9 m + 11sm	2A	13.90 ± 0.59	24.19 ± 1.43
H. apenninum (L.) Mill. subsp. *apenninum*	10	239	5.81	6	37.38	9.82	10 m + 10sm	2A	16.27 ± 0.76	25.89 ± 1.25
H. apenninum subsp. *stoechadifolium* (Brot.) Samp.	10	236	7.36	14	41.78	7.53	12 m + 8sm	2A	13.29 ± 0.51	22.93 ± 0.70
H. bramwelliorum Marrero Rodr.	10	412	4.96	7	30.38	6.10	10 m + 10sm	2A	14.77 ± 0.53	23.89 ± 0.79
H. broussonetii Dunal	10	397, 432	4.98	5	24.18	2.97	8 m + 12sm	2A	12.06 ± 1.32	24.59 ± 0.47
H. bystropogophyllum Svent.	10	419	4.74	5	24.84	8.43	13 m + 7sm	2A	12.59 ± 1.10	24.00 ± 1.08
H. cirae A.Santos	10	432	5.23	11	30.49	9.71	12 m + 8sm	2A	13.92 ± 1.01	22.86 ± 1.80
H. croceum (Desf.) Pers	10	573	6.56	13	38.15	8.47	12 m + 8sm	2A	13.66 ± 0.50	22.28 ± 1.08
H. fontqueri Sennen	10	41	5.72	9	37.63	4.80	11 m + 9sm	2A	15.78 ± 0.75	23.59 ± 0.71
H. gonzalezferreri Marrero Rodr.	10	411	4.93	9	31.88	7.07	12 m + 8sm	1A	13.42 ± 0.53	22.66 ± 1.05
H. grosii Pau & Font Quer	10	425	7.52	9	37.63	5.85	9 m + 11sm	2A	17.13 ± 0.70	23.04 ± 0.81
H. guerrae Sánchez-Gómez, J.S.Carrion & M.A. Carrión *	10	762	5.68	8	37.00	5.86	12 m + 8sm	2A	15.60 ± 0.69	24.87 ± 0.66
H. helianthemoides (Desf.) Grosser	10	426, 429	7.22	8	34.64	5.89	10 m + 10sm	2A	13.89 ± 0.93	27.66 ± 1.07

(*continued on next page*)

Table 1 (*continued*)

	n =	ID	2C	N	THL	CV	Karyotype formula	Stebbins' Karyotype asymmetry	CV_{CL} ± SE	M_{CA} ± SE
H. henriquezii A.Rebolé, A.Acevedo & A.García	10	432	4.52	7	27.04	7.49	10 m + 10sm	2A	13.61 ± 0.79	24.46 ± 0.79
H. hirtum (L.) Mill.	10	431	5.50	14	35.47	5.87	13 m + 7sm	2A	13.93 ± 0.53	22.61 ± 0.37
H. inaguae Marrero Rodr., González-Mart. & González-Art.	10	418	5.41	10	31.86	9.24	10 m + 10sm	2A	12.90 ± 0.76	22.92 ± 0.49
H. juliae Wildpret	10	434	4.70	5	24.09	7.04	13 m + 7sm	2A	18.70 ± 0.35	26.04 ± 1.09
H. kotschyanum Boiss.	10	646	10.56	10	47.84	8.37	6 m + 10sm + 4st	2A	18.55 ± 0.34	30.20 ± 0.54
H. linii A.Santos	10	399	4.96	9	30.33	8.96	10 m + 10sm	2A	12.44 ± 0.64	22.64 ± 0.89
H. marminorense Alcaraz, Peinado & Mart. Parras	10	276	5.46	10	35.25	9.60	10 m + 10sm	2A	13.94 ± 0.98	24.16 ± 1.02
H. morisianum Bertol.	10	574	6.30	9	36.91	5.02	12 m + 8sm	2A	13.03 ± 0.47	20.69 ± 0.66
H. neopiliferum Muñoz Garm. & Navarro	10	309	6.03	11	36.97	8.87	11 m + 9sm	2A	14.08 ± 0.55	23.26 ± 0.59
H. nummularium (L.) Mill. *nummularium*	10	575	6.78	13	38.31	8.55	10 m + 10sm	2A	13.25 ± 0.73	24.15 ± 1.03
H. nummularium subsp. *cantabricum* (M.Laínz) Martín-Hernanz, Velayos, Albaladejo & Aparicio	10	373	6.25	7	37.68	4.94	12 m + 8sm	2A	13.96 ± 0.67	23.21 ± 0.86
H. nummularium subsp. *tinetense* (M.Mayor & Fern. Benito) Martín-Hernanz, Velayos, Albaladejo & Aparicio	10	369	7.47	10	40.53	8.20	11 m + 9sm	2A	14.25 ± 0.52	25.30 ± 0.95
H. obtusifolium Dunal *	10	737	10.06	8	47.95	4.34	6 m + 8sm + 6st	3A	18.21 ± 0.91	33.89 ± 0.41
H. pergamaceum Pomel	10	114	6.47	10	34.83	7.79	10 m + 10sm	2A	12.39 ± 0.87	22.81 ± 0.56
H. polygonoides Peinado, Mart.Parras, Alcaraz & Espuelas *	10	710	6.72	13	38.73	8.04	10 m + 10sm	2A	13.70 ± 0.67	28.22 ± 0.94
H. raskebdanae Alonso, Crespo, Juan & Sáez	10	274	5.99	8	34.96	5.20	9 m + 11sm	2A	13.91 ± 0.46	24.98 ± 1.37
H. ruficomum (Viv.) Spreng.	10	111	6.07	9	36.23	8.66	7 m + 13sm	2A	13.32 ± 0.39	26.20 ± 0.74
H. sauvagei Raynaud	10	282	7.19	13	39.81	6.23	8 m + 12sm	2A	18.14 ± 0.21	25.73 ± 0.52
H. sp. nov. 1	10	405	4.46	6	30.08	9.89	6 m + 14sm	2A	16.06 ± 1.34	29.38 ± 1.17
H. teneriffae Coss.	10	401	4.81	6	26.49	9.72	11 m + 7sm + 2st	2A	14.20 ± 0.81	25.50 ± 1.25
H. tholiforme Bramwell, Ortega & Navarro	10	420	4.84	5	26.80	4.92	6 m + 14sm	2A	11.07 ± 0.83	27.45 ± 1.60
H. tibiabinae Marrero Rodr., Díaz Bertrana & S. Scholz	10	437	4.99	10	29.86	7.04	11 m + 9sm	2A	15.49 ± 1.94	24.44 ± 1.22
H. vesicarium Boiss.	10	641	8.22	10	40.12	8.11	12 m + 8sm	2A	12.75 ± 0.60	17.92 ± 0.63
H. violaceum (Cav.) Pers.	10	81, 364	5.83	13	37.07	8.46	9 m + 11sm	2A	13.43 ± 0.57	24.41 ± 0.989
H. virgatum (Desf.) Pers.	10	111, 424	6.63	8	38.54	9.94	10 m + 10sm	2A	12.40 ± 0.66	25.38 ± 0.65
H. viscarium Boiss. & Reut.	10	41, 275	5.60	7	37.03	7.22	8 m + 12sm	2A	14.44 ± 0.30	27.25 ± 1.35

(Table S1). After quality filtering, an average of 3.76 million paired-end reads per sample was retained (range: 690,898–11.5 million), with a mean enrichment efficiency of 26.0% (5.8–52.2%). Assemblies included, on average, 308 genes per sample reaching at least 50% of the target length, amounting to approximately 235 kb of nuclear data per sample (range: 174–267 kb), representing ~ 81.9% recovery relative to the target file. Eight samples and five genes were excluded due to poor coverage or low representation.

The concatenated phylogenetic analysis in IQ-TREE provided strong support for relationships across the genus, with bootstrap values ≥ 95% for most nodes (Fig. S3). The coalescent-based analysis in ASTRAL-III (Fig. S4) yielded a largely congruent topology, with high local posterior probabilities for most deep and intermediate nodes. Both approaches were consistent with each other and with previous phylogenetic reconstructions based on Sanger sequencing (Aparicio et al., 2017) and GBS data (Martín-Hernanz et al., 2021a), supporting the monophyly of the three subgenera and the ten currently recognized sections, as well as the relationships among them. Relationships among species were generally well supported and concordant between methods, although the coalescent analysis showed slightly lower resolution at terminal nodes. Gene tree discordance was especially high in sections *Pseudocistus* Dunal and *Helianthemum*, indicating lower congruence among loci in these lineages.

Divergence time estimates using TreePL placed the stem age of *Helianthemum* at approximately 19.6 Ma (early Miocene), and the crown age at 13.2 Ma. The three major subgenera diverged shortly thereafter: subg. *Eriocarpum* around 8.5 Ma, subg. *Plectolobum* at ~ 7.0 Ma, and subg. *Helianthemum* at ~ 6.9 Ma (Fig. S5). Most species-level diversification occurred within the last 4 million years, during the late Pliocene and Pleistocene.

3.2. Genome size variation and karyotype descriptors

We conducted flow cytometry analyses for 282 samples, including 268 individuals from 83 *Helianthemum* taxa. All genome size estimates show high analytical quality, with coefficient of variation (CV) below 5% in every case except *H. confertum* Dunal (CV = 5.18%). 2C values range from 1.65 ± 0.02 pg in *H. sessiliflorum* (Desf.) Pers. to 10.60 ± 0.42 pg in *H. kotschyanum* Boiss., representing a 6.5-fold difference across the genus. Intraspecific variation is low, but values covered a broad spectrum: 15 taxa (18.3%) had very small genomes, 54 (65.9%) small genomes, and 13 (15.9%) intermediate genome sizes, following established categorisation thresholds (Table 1).

Illustrative metaphase spreads of the newly added species in this paper are in Fig. S2. We analysed a total of 743 mitotic metaphase plates, yielding an average of 9.06 ± 0.09 (mean ± SE) measurements per species. Chromosome numbers are highly conserved across the genus, predominantly 2n = 20 or 22, with only rare deviations such as 2n = 10 in *H. squamatum* and 2n = 24 in *H. caput-felis* Boiss. (Fig. 2).

Total haploid karyotype length (THL) shows substantial interspecific variation across *Helianthemum*, ranging from 16.91 μm in *H. sessiliflorum* to 47.95 μm in *H. obtusifolium*, representing nearly a three-fold difference. The genus-wide mean THL was 31.62 μm. Section-level means range from 18.93 to 44.03 μm, and subgenus-level means from 22.39 to 38.27 μm (Table 1).

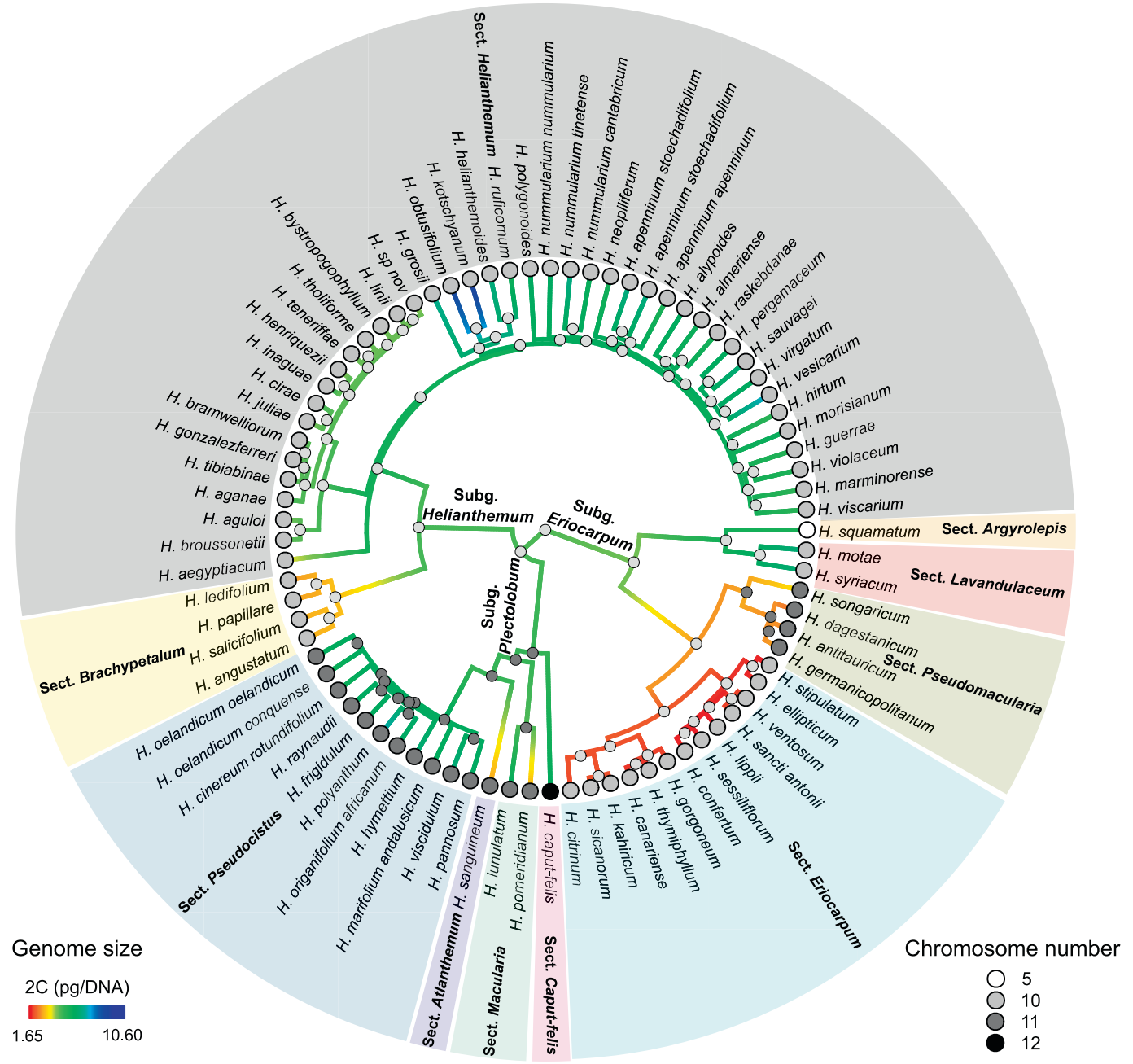

Fig. 2. Genome size (2C values, pg DNA) reconstructed as a continuous trait across the time-calibrated phylogeny of *Helianthemum*. Branch colors indicate reconstructed genome size values (range: 1.65–10.60 pg). Circles at tips and internal nodes represent haploid chromosome numbers (n), based on the updated ancestral chromosome numbers reconstruction. Taxon names follow the nomenclature proposed by Martín-Hernanz et al. (2021a). Taxonomic sections are highlighted as colored arcs around the outer ring. For clarity, the phylogeny was pruned to strictly retain the subset of 82 taxa with complete empirical data for both genome size and chromosome number.

In contrast, karyotype asymmetry indices show little variation across the genus. Interspecific CV_{CL} values range from 9.48 to 29.95, and M_{CA} values from 10.91 to 33.32. These indices are also relatively stable within major lineages, with section-level CV_{CL} values ranging from 12.69 to 21.73 and M_{CA} from 10.91 to 28.06, and subgenus-level values from 14.30 to 16.73 (CV_{CL}) and 20.23–23.93 (M_{CA}).

3.3. Genome size evolution and correlation with karyotype descriptors

Genome size exhibits strong phylogenetic structure. Blomberg's K was high (K = 2.20, p = 0.001), indicating that closely related species resemble each other more than expected under a Brownian model. Pagel's λ was effectively equal to one (λ = 0.9999, $p < 1 \times 10^{-38}$), showing that trait covariation closely matches the topology and branch lengths of the phylogeny. Model comparison based on AICc favours an Early-Burst (EB) model (AICc = –202.61) over Brownian motion (BM; ΔAICc = 9.30), Ornstein–Uhlenbeck with a single optimum (OU; ΔAICc = 11.46), and white-noise (WN; ΔAICc > 170). The EB model implies higher rates of genome-size evolution early in the diversification of the genus and lower rates toward the present.

The ancestral 2C value at the crown node of *Helianthemum* is 5.04 pg (95% CI: 3.28–6.80), a mid-value within the extant genome-size range (1.65–10.60 pg). Most lineages retain values close to this ancestral state, but several clades show clear reductions towards very small genomes (2C < 4 pg). A major decrease takes place at the ancestral node giving rise to sect. *Pseudomacularia* Grosser and sect. *Eriocarpum*, with additional reductions in sect. *Atlanthemum* (Raynaud) G.López, Ortega Oliv. and Romero García, sect. *Brachypetalum* Dunal, and in isolated species such as *H. pomeridianum* Dunal (sect. *Macularia* Dunal) and *H. aegyptiacum* (sect. *Helianthemum*). In contrast, genome-size increases are rare and restricted to the lineage leading to *H. obtusifolium* and *H. kotschyanum*, which reached intermediate GS values (2C > 10 pg). Overall, the reconstruction reveals a predominantly conservative pattern, with asymmetric deviation from the ancestral state characterised by multiple independent reductions and only a single instance of genome expansion.

Phylogenetically informed regressions (PGLS) reveal a strong positive association between GS and THL, indicating that both traits covary and can be considered tightly linked (Fig. 3). In contrast, we found no significant correlations between GS and chromosome number or with either interchromosomal (CV_{CL}) and intrachromosomal (M_{CA}) asymmetry indices, suggesting that GS variation is largely decoupled from both chromosomal number and karyotype architecture (Table 2).

3.4. Chromosome number evolution

The reconstruction of chromosome-number evolution using ChromEvol v3.0 strongly supports a heterogeneous-rate model, which outperformed the null homogeneous model (HOMOGENEOUS: AICc = 75.27; HETEROGENEOUS model: AICc = 59.01; ΔAICc = 16.26). This substantial difference indicates that rates of chromosome evolution are not uniform across the phylogeny.

The best-fitting model identifies a single major rate shift, corresponding to a hotspot of accelerated dysploidy on the branch leading to *H. squamatum* (n = 5). In the background phylogeny (model 1), the rate

Table 2
Univariate results of phylogenetic generalized least square (PGLS) regressions assessing the relationship between genome size and karyotype descriptors (in log scale). THL = total haploid (monoploid) karyotype length; CV_{CL} = coefficient of variation in chromosome length; M_{CA} = mean centromeric asymmetry. SE = standard error.

Karyotype descriptor	Estimate	SE	*P*-value
Chromosome number	0.0990	0.3468	0.7760
THL	**1.0165**	**0.0890**	**< 0.001**
CV_{CL}	−0.1212	0.1289	0.3499
M_{CA}	−0.0778	0.1439	0.5906

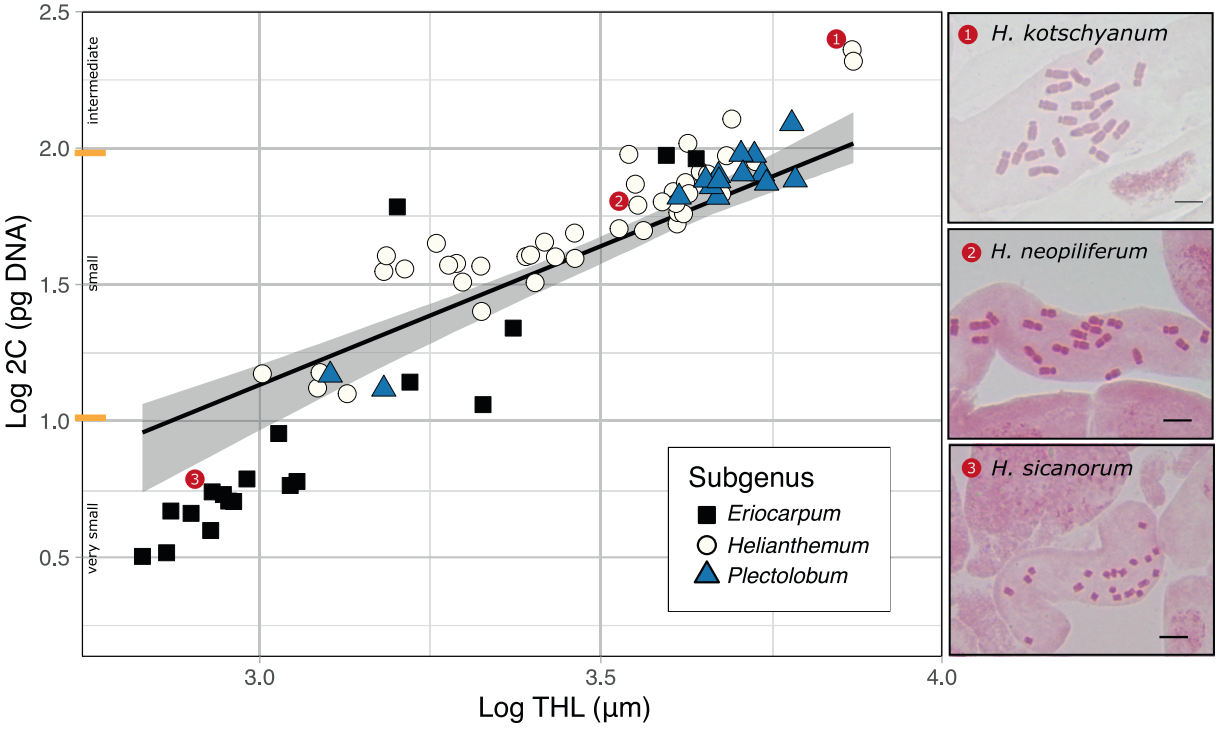

Fig. 3. Phylogenetically informed correlation (PGLS) between log-transformed 2C-values (GS) and total haploid karyotype length (THL) for the studied species of *Helianthemum*. Thresholds of GS categorization following Leitch et al. (1998) are indicated in Y axe. For illustration, chromosome spreads of *H. sicanorum* Brullo, Giusso & Sciandr. (very small genome size), *H. neopiliferum* Muñoz Garm. & Navarro (small genome size) and *H. kotschyanum* Boiss. (intermediate genome size) are included. 95% confidence interval of parameter estimation is shown on the regression line. Scale bars = 5 µm.

of chromosome loss (ρ) is essentially zero ($2.4 \times 10^{-1^{0}}$), consistent with the high stability of chromosome numbers in the genus (n = 10, 11). By contrast, the derived hotspot clade (model 2) shows a marked increase in both aneuploidy parameters: the loss rate (ρ) rises from ~ 0 to 0.56 events My^{-1}, and the gain rate (λ) increased from 0.015 to 0.35 gain events My^{-1}. This coordinated acceleration, particularly the sharp rise in chromosome loss, pinpoints *H. squamatum* as the origin of the only abrupt dysploid transition detected in the genus.

4. Discussion

Our results provide the first genus-wide assessment of genome size evolution in *Helianthemum* within the context of a comprehensive Angiosperms353 phylogenetic framework, which offers far greater taxonomic and geographic resolution than previous reconstructions. Earlier studies had shown that chromosome numbers and overall karyotype structure are remarkably conserved across the genus, with most species exhibiting stable diploid complements and predominantly metacentric to submetacentric chromosomes (Aparicio et al., 2019; Martín-Hernanz et al., 2023b). By integrating these karyological data with genome size estimates for c. 75% of the species within a densely sampled time-calibrated phylogeny, we show that this chromosomal stasis contrasts sharply with a dynamic evolution of nuclear DNA content (Fig. 2).

4.1. Genome size and karyotype variation

A primary aim of this study was to quantify the extent of genome size variation across *Helianthemum* (Objective i) and evaluate its relationship with key karyotype descriptors (Objective iii). We found that genome size varies 6.5-fold across *Helianthemum*, yet chromosome numbers remain almost invariant (n = 5, 10, 11 or 12) and karyotype architecture shows only minimal differentiation among lineages (Table 1). Such a marked decoupling between genome size dynamics and chromosomal stability is uncommon among angiosperms. In many plant groups, shifts in genome size are tightly linked to polyploidy, dysploidy or changes in karyotype symmetry (Leitch and Bennett, 2004; Weiss-Schneeweiss and Schneeweiss, 2013; Pellicer et al., 2018). However, this relationship is not always straightforward; for instance, recent broad-scale analyses in grasses have revealed highly complex evolutionary dynamics where dysploid changes lack a simple causal relationship with genome size shifts, including rare patterns of concurrent genome downsizing (Tkach et al., 2025). Even in lineages with stable chromosome numbers, genome size evolution often accompanies structural rearrangements, as observed in *Lilium* (Peruzzi et al., 2009), *Hieracium* (Chrtek et al., 2009) or *Orobanche* (Weiss-Schneeweiss et al., 2006). In contrast, *Helianthemum* resembles the pattern found in *Anacyclus* (Vitales et al., 2020) and certain orchid lineages (Moraes et al., 2022), where substantial genome size diversification occurs despite highly conserved karyotypes. This combination of genomic flexibility and karyotypic rigidity positions *Helianthemum* as a valuable model for investigating how genome size can evolve independently of major chromosomal restructuring.

The strong association between genome size and total haploid length (Fig. 3) confirms that variation in nuclear DNA content is accommodated through proportional changes in chromosome length (Levin, 2002; Leitch and Caparelli, 2009; Lacerda et al., 2019). This pattern corroborates previous infrageneric results (Martín-Hernanz et al., 2023b) and supports THL as a reliable cytological proxy for genome size, particularly in lineages with stable chromosome numbers (Medeiros-Neto et al., 2017). Although metaphase chromosome condensation may introduce technical variation in THL measurements, the observed variation is biologically meaningful given the consistency of the relationship across species in our study. Moreover, Fig. 3 shows that in *Helianthemum*, most "very small" genomes fall below the regression line and outside the 95% confidence interval. This pattern may provide new evidence for increased chromosome condensation or spiralization during mitosis, a phenomenon that appears to be more pronounced in smaller genomes (Kramer et al., 2021).

In contrast, genome size does not correlate with chromosome number or with intra- and interchromosomal asymmetry (M_{CA}, CV_{CL}), both of which remain remarkably invariant across the genus. This stability indicates that genome size diversification has not involved detectable shifts in centromere position or arm ratios, supporting the absence of large-scale structural remodelling of the karyotype (Techio et al., 2010; Peruzzi and Eroğlu, 2013). Instead, genome size variation is more plausibly driven by quantitative turnover of repetitive DNA, a major force in genome evolution (Bennetzen and Kellogg, 1997; Pellicer et al., 2018). Likely mechanisms include the differential amplification or loss of transposable elements and satellite repeats (Vitales et al., 2020; Sader et al., 2021) and small deletions mediated by illegitimate recombination (Devos et al., 2002; Moreno-Aguilar et al., 2022).

4.2. Genome size evolution

An important goal of this study was to understand the macroevolutionary dynamics of genome size across the genus (Objective ii). Our phylogenetic analyses indicate that genome size in *Helianthemum* follows an early-burst (EB) mode of evolution. Strong support for the EB model over Brownian Motion, Ornstein–Uhlenbeck and white-noise alternatives, together with high values of Blomberg's K (2.20) and Pagel's λ (≈1), reveals pronounced phylogenetic structure and a temporal decline in evolutionary rates. Most extant genome-size diversity appears to have originated early in the diversification of the genus, with later lineages retaining these values and evolving at markedly slower rates. This early diversification is visually captured by the continuous character mapping (Fig. 2), which illustrates that some of the most abrupt shifts occurred in deeper branches, such as the divergence between sects. *Pseudomacularia* and *Eriocarpum*, or at the base of sect. *Brachypetalum*. Similar time-dependent declines in genome-size evolution have been observed only rarely (e.g. *Orobanche*: Weiss-Schneeweiss et al., 2006) but align with the general tendency of genome size to show strong phylogenetic signal in many angiosperm clades (Andrés-Sánchez et al., 2013; Beaulieu et al., 2007; Bureš and Ozcan, 2023; Cacho et al., 2021). The reconstructed ancestral genome size (~5.04 pg) lies within the mid-range of contemporary values, from which several asymmetric transitions occurred. Most represent genome downsizing, whereas only one lineage (*H. obtusifolium–H. kotschyanum*) shows a modest increase, consistent with a directional bias towards genome reduction and subsequent evolutionary conservatism.

Although ecological correlates of genome size were not explicitly tested here, some phylogenetic clustering hints at potential ecological or life-history influences. Unlike many geophytic lineages—where massive genome expansions are often linked to nutrient storage strategies (Veselý et al., 2012)—or long-lived trees that tend to exhibit constrained genomes with slow evolutionary rates (Pellicer et al., 2018), the rapid diversification of short-lived shrubs and annuals in *Helianthemum* offers a highly dynamic scenario. Indeed, these distributions mirror broader patterns in angiosperms, seemingly aligning with the Large Genome Constraint Hypothesis (Knight et al., 2005), where small genomes are associated with rapid development, metabolic efficiency and stress tolerance (Bennett, 1987; Knight and Ackerly, 2002; Cacho et al., 2021; Bureš et al., 2024). In *Helianthemum*, very small genomes appear to be associated with species adapted to semi-arid and subdesert environments (sects. *Pseudomacularia*, *Eriocarpum*; *H. pomeridianum*) or insular habitats (Canary Islands clade, Aparicio et al., 2017), as well as with annual lineages (sects. *Atlanthemum*, *Brachypetalum*; *H. aegyptiacum*), a pattern previously documented using THL data (Martín-Hernanz et al., 2023b). While such parallels are intriguing, establishing causation will require explicit comparative analyses integrating ecological, functional and genomic predictors.

4.3. Chromosome number evolution

A final aim of this study was to reassess chromosome-number evolution to determine the patterns and rates of dysploid change in the genus (Objective iv). In this regard, chromosome-number evolution in *Helianthemum* also aligns with strong cytogenetic conservatism. Our ChromEvol 3.0 analyses, consistent with earlier reconstructions, indicate extremely low rates of single-chromosome gains and losses across the genus, with a single notable deviation: the terminal branch leading to *H. squamatum* (n = 5), which shows accelerated descending dysploidy. Yet even in this lineage, genome size remains comparatively large (80% of its sister species *H. syriacum*), reinforcing that descending dysploidy does not necessarily entail drastic genome downsizing (Luo et al., 2009; Mandáková and Lysák, 2018).

5. Conclusions

This study addresses the four questions outlined in the Introduction by integrating genome-size estimates, updated karyotype descriptors and a nearly complete Angiosperms353 phylogeny. First, we show that genome size exhibits extensive and unevenly distributed variation across *Helianthemum*. Second, comparative modelling reveals that this diversity originated largely early in the genus, following an early-burst dynamic with strong phylogenetic structure. Third, we demonstrate that genome size correlates tightly with total haploid karyotype length but is decoupled from chromosome number and karyotype asymmetry, indicating that genome-size diversification occurred without major chromosomal rearrangements. Finally, by reassessing chromosome-number evolution, we confirm the extreme stability of the karyotype, with only a single abrupt dysploid reduction and very few minor changes.

Together, these results show that genome-size evolution in *Helianthemum* is driven primarily by lineage-specific processes of DNA gain and loss acting within a long-term conserved chromosomal framework. This combination of dynamic genomes and stable karyotypes positions *Helianthemum* as an exceptional model for understanding how genome size evolves in the absence of large-scale chromosomal restructuring. While this study establishes a robust macroevolutionary framework for genome size evolution, it is currently limited by the absence of explicit environmental modelling and sequence-level data for repetitive elements. Future analyses integrating repetitive-DNA composition, ecological gradients and life-history traits will clarify the drivers of genome-size shifts in this lineage.

6. Declaration of generative AI and AI-assisted technologies in the manuscript preparation process

During the preparation of this manuscript, the authors used ChatGPT in order to improve clarity and English style in several sections. After using this tool, the authors thoroughly reviewed and edited the content as needed and take full responsibility for the content of the published article.

CRediT authorship contribution statement

Sara Martín-Hernanz: Writing – review & editing, Writing – original draft, Visualization, Validation, Supervision, Software, Resources, Methodology, Investigation, Formal analysis, Data curation, Conceptualization. **Rafael G. Albaladejo:** Writing – review & editing, Project administration, Methodology, Funding acquisition, Formal analysis, Conceptualization. **Juan Viruel:** Writing – review & editing, Methodology, Conceptualization. **Rafael Matos:** Writing – review & editing, Formal analysis. **Sara Brito Lopes:** Writing – review & editing, Formal analysis. **Encarnación Rubio:** Data curation. **Mariana Castro:** Writing – review & editing, Methodology, Formal analysis. **João Loureiro:** Writing – review & editing, Methodology, Formal analysis. **Polina Volkova:** Writing – review & editing, Resources. **Abelardo Aparicio:** Writing – review & editing, Writing – original draft, Visualization, Resources, Project administration, Methodology, Investigation, Funding acquisition, Formal analysis, Data curation, Conceptualization.

Funding

This work was supported by grants CGL2017-82465-P and PID2020-116355GB-I00 from the Spanish Ministerio de Economía y Competitividad to AA, and PID2020-116355GB-I00 from the Spanish Ministerio de Ciencia e Innovación to RGA, all administered by the University of Seville; and by the state assignment of the Papanin Institute for Biology of Inland Waters, RAS (theme 124032100076-2) to PV. Open Access funding provided by Universidad Complutense de Madrid.

Declaration of competing interest

The authors declare that they have no known competing financial interests or personal relationships that could have appeared to influence the work reported in this paper.

Acknowledgements

We thank Miguel Ángel Copete Carreño (Universidad de Castilla-La Mancha) and Anthemis Melifronidou (Plant Health and Marketing Standards of Agricultural Products Sector, Department of Agriculture from Cyprus) for providing seeds of *H. polygonoides* and *H. obtusifolium* respectively for this study. We also thank Dr. I.A. Schanzer, curator of MHA herbarium, for providing samples of *H. zheguliense* and *H. baschkirorum*. Finally, we thank all the collectors (listed in Table S1 and Table S2) for providing material.

Appendix A. Supplementary data

Supplementary data to this article can be found online at https://doi.org/10.1016/j.ympev.2026.108627.

Data availability

All sequencing data are in NCBI SRA (PRJNA1219060). The phylogenomic dataset is publicly available on Zenodo (DOI: 10.5281/zenodo.17050311).

References

Altinordu, F., Peruzzi, L., Yu, Y., He, X., 2016. A tool for the analysis of chromosomes: KaryoType. Taxon 65, 586–592. https://doi.org/10.12705/653.9.

Andrés-Sánchez, S., Temsch, E., Rico, E., Martínez-Ortega, M.M., 2013. Genome size in *Filago* L. (Asteraceae, Gnaphalieae) and related genera: phylogenetic, evolutionary and ecological implications. Plant Syst. Evol. 299, 331–345. https://doi.org/10.1007/s00606-012-0724-3.

Aparicio, A., Escudero, M., Valdés-Florido, A., Pachón, M., Rubio, E., Albaladejo, R.G., Martín-Hernanz, S., Pradillo, M., 2019. Karyotype evolution in *Helianthemum* (Cistaceae): dysploidy, achiasmate meiosis and ecological specialization in *H. squamatum*, a true gypsophile. Bot. J. Linn. Soc. 191, 484–501. https://doi.org/10.1093/botlinnean/boz066.

Aparicio, A., Martín-Hernanz, S., Parejo-Farnés, C., Arroyo, J., Yeşilyurt, E.B., Yeşilyurt, M.-L., Rubio, E., Albaladejo, R.G., 2017. Phylogenetic reconstruction of the genus *Helianthemum* (Cistaceae) using plastid and nuclear DNA sequences: systematic and evolutionary inferences. Taxon 66, 964–984. https://doi.org/10.12705/664.5.

Beaulieu, J.M., Moles, A.T., Leitch, I.J., Bennett, M.D., Dickie, J.B., Knight, C.A., 2007. Correlated evolution of genome size and seed mass. New Phytol. 173, 422–437. https://doi.org/10.1111/j.1469-8137.2006.01919.x.

Bennett, M.D., 1987. Variation in genomic form in plants and its ecological implications. New Phytol. 106, 177–200. https://doi.org/10.1111/j.1469-8137.1987.tb04689.x.

Bennetzen, J.L., Kellogg, E.A., 1997. Do plants have a one-way ticket to genomic obesity? Plant Cell 9, 1509–1514. https://doi.org/10.1105/tpc.9.9.1509.

Bennetzen, J.L., Ma, J., Devos, K.M., 2005. Mechanisms of recent genome size variation in flowering plants. Ann. Bot. 95, 127–132. https://doi.org/10.1093/aob/mci008.

Blomberg, S.P., Garland, T.J., Ives, A.R., 2003. Testing for phylogenetic signal in comparative data: behavioral traits are more labile. Evolution 57, 717–745. https://doi.org/10.1111/j.0014-3820.2003.tb00285.x.

Bolger, A.M., Lohse, M., Usadel, B., 2014. Trimmomatic: a flexible trimmer for Illumina sequence data. Bioinformatics 30, 2114–2120. https://doi.org/10.1093/bioinformatics/btu170.

Bureš, P., Elliott, T.L., Veselý, P., Šmarda, P., Forest, F., Leitch, I.J., Lughadha, E.N., Soto Gomez, M., Pironon, S., Brown, M.J.M., Zedek, Š.F., 2024. The global distribution of angiosperm genome size is shaped by climate. New Phytol. 243, 217–231. https://doi.org/10.1111/nph.19544.

Bureš, P., Ozcan, M., et al., 2023. Evolution of genome size and GC content in the tribe Carduinae (Asteraceae): rare descending dysploidy and polyploidy, limited environmental control, and strong phylogenetic signal. Preslia 95, 185–213. https://doi.org/10.23855/preslia.2023.185.

Cacho, N.I., McIntyre, P.J., Kliebenstein, D.J., Strauss, S.Y., 2021. Genome size evolution is associated with climate seasonality and glucosinolates, but not life history, soil nutrients or range size, across a clade of mustards. Ann. Bot. 127, 887–902. https://doi.org/10.1093/aob/mcab028.

Capella-Gutiérrez, S., Silla-Martínez, J.M., Gabaldón, T., 2009. trimAl: a tool for automated alignment trimming in large-scale phylogenetic analyses. Bioinformatics 25, 1972–1973. https://doi.org/10.1093/bioinformatics/btp348.

Carta, A., Peruzzi, L., 2015. Testing the large genome constraint hypothesis: plant traits, habitat and climate seasonality in Liliaceae. New Phytol. 210, 709–716. https://doi.org/10.1111/nph.13769.

Chrtek Jr., J., Zahradníček, J., Krak, K., Fehrer, J., 2009. Genome size in Hieracium subgenus Hieracium (Asteraceae) is strongly correlated with major phylogenetic groups. Ann. Bot. 104, 161–178. https://doi.org/10.1093/aob/mcp107.

Devos, K.M., Brown, J.K.M., Bennetzen, J.L., 2002. Genome size reduction through illegitimate recombination counteracts genome expansion in *Arabidopsis*. Genome Res. 12 (7), 1075–1079.

Doležel, J., Greilhuber, J., Suda, J., 2007. Estimation of nuclear DNA content in plants using flow cytometry. Nat. Protoc. 2, 2233–2244. https://doi.org/10.1038/nprot.2007.310.

Doyle, J.J., Doyle, J.L., 1987. A rapid DNA isolation procedure for small quantities of fresh leaf tissue. Phytochemical Bulletin 19, 11–15.

Drummond, A.J., Rambaut, A., 2007. BEAST: Bayesian evolutionary analysis by sampling trees. BMC Evol. Biol. 7, 214. https://doi.org/10.1186/1471-2148-7-214.

Du, Y., Bi, Y., Zhang, M., Yang, F., Jia, G., Zhang, X., 2017. Genome size diversity in *Lilium* (Liliaceae) is correlated with karyotype and environmental traits. Front. Plant Sci. 8, 1303. https://doi.org/10.3389/fpls.2017.01303.

Elliott, T.L., Zedek, F., Barrett, R.L., Bruhl, J.J., Escudero, M., Hroudová, Z., Joly, S., Larridon, I., Luceño, M., Márquez-Corro, J.I., Martín-Bravo, S., Muasya, A.M., Šmarda, P., Thomas, W.W., Wilson, K.L., Bureš, P., 2022. Chromosome size matters: genome evolution in the cyperid clade. Ann. Bot. 130, 999–1014. https://doi.org/10.1093/aob/mcac136.

Garnatje, T., Vallès, J.M., García, S., Hidalgo, O., Sanz, M., Candela, M.A., Siljak-Yakovlev, S., 2004. Genome size in *Echinops* L. and related genera (Asteraceae, Cardueae): karyological, ecological and phylogenetic implications. Biological Cell 96, 117–124. https://doi.org/10.1016/j.biolcel.2003.11.005.

Greilhuber, J., Doležel, J., Lysak, M.A., Bennett, M.D., 2005. The origin, evolution and proposed stabilization of the terms 'genome size' and 'C-value' to describe nuclear DNA contents. Ann. Bot. 95 (1), 255–260. https://doi.org/10.1093/aob/mci019.

Harmon, L.J., Weir, J.T., Brock, C.D., Glor, R.E., Challenger, W., 2008. GEIGER: investigating evolutionary radiations. Bioinformatics 24, 129–131. https://doi.org/10.1093/bioinformatics/btm538.

Hawkins, J.S., Hu, G., Rapp, R.A., Grafenberg, J.L., Wendel, J.F., 2008. Phylogenetic determination of the pace of transposable element proliferation in plants: copia and LINE-like elements in Gossypium. Genome 5, 11–18. https://doi.org/10.1139/G07-099.

Ho, L.S.T., Ané, C., 2014. A linear-time algorithm for Gaussian and non-Gaussian trait evolution models. Syst. Biol. 63, 397–408. https://doi.org/10.1093/sysbio/syu005.

Hoang, D.T., Chernomor, O., von Haeseler, A., Minh, B.Q., Vinh, L.S., 2018. UFBoot2: improving the ultrafast bootstrap approximation. Mol. Biol. Evol. 35, 518–522. https://doi.org/10.1093/molbev/msx281.

Johnson, M.G., Gardner, E.M., Liu, Y., Medina, R., Goffinet, B., Shaw, A.J., Zerega, N.J. C., Wickett, N.J., 2016. HybPiper: extracting coding sequence and introns for phylogenetics from high-throughput sequencing reads using target enrichment. App. Plant Sci. 4, 1600016. https://doi.org/10.3732/apps.1600016.

Johnson, M.G., Pokorny, L., Dodsworth, S., Botigué, L.R., Cowan, R.S., Devault, A., Eisenhardt, W.L., Epitaealage, N., Forest, F., Kim, J.T., Leebens-Mack, J.H., Leitch, I. J., Maurin, O., Soltis, D.E., Soltis, P.S., Wong, G.K., Baker, W.J., Wickett, N.J., 2019. A universal probe set for targeted sequencing of 353 nuclear genes from any flowering plant designed using k-medoids clustering. Syst. Biol. 68, 594–606. https://doi.org/10.1093/sysbio/syy086.

Katoh, K., Misawa, K., Kuma, K., Miyata, T., 2002. MAFFT: a novel method for rapid multiple sequence alignment based on fast Fourier transform. Nucleic Acids Res. 30, 3059–3066. https://doi.org/10.1093/nar/gkf436.

Knight, C.A., Molinari, N.A., Petrov, D.A., 2005. The large genome constraint hypothesis: evolution, ecology and phenotype. Ann. Bot. 95, 177–190. https://doi.org/10.1093/aob/mci011.

Knight, C.A., Ackerly, D.D., 2002. Variation in nuclear DNA content across environmental gradients: a quantile regression analysis. Ecol. Lett. 5, 66–76. https://doi.org/10.1046/j.1461-0248.2002.00283.x.

Kück, P., Meusemann, K., 2010. FASconCAT: convenient handling of data matrices. Mol. Phylogenet. Evol. 56, 1115–1118. https://doi.org/10.1016/j.ympev.2010.04.024.

Kramer, E.M., Tayjasanant, P.A., Cordone, B., 2021. Scaling laws for mitotic chromosomes. Front. Plant Sci. 9, 684278. https://doi.org/10.3389/fcell.2021.684278.

Lacerda, M.M., Silva, J.C., Vieira, A.T., Clarindo, W.R., 2019. Cytogenetic characterization of Passiflora megacoriacea K. Port.-Utl. employing image cytometry. Cytologia 84, 353–357. https://doi.org/10.1508/cytologia.84.353.

Leitch, I.J., Bennett, M.D., 2004. Genome downsizing in polyploid plants. Biol. J. Linn. Soc. 82, 651–663. https://doi.org/10.1111/j.1095-8312.2004.00349.x.

Leitch, I.J., Chase, M.W., Bennett, M.D., 1998. Phylogenetic analysis of DNA C-values provides evidence for a small ancestral genome size in flowering plants. Ann. Bot. 82, 85–94. https://doi.org/10.1006/anbo.1998.0783.

Levan, A., Fredga, K., Sandberg, A.A., 1964. Nomenclature for centromeric position on chromosomes. Hereditas 52, 201–220. https://doi.org/10.1111/j.1601-5223.1964.tb01953.x.

Levin, D.A., 2002. The role of chromosomal change in plant evolution. Oxford University Press.

Loureiro, J., Rodriguez, E., Dolezel, J., Santos, C., 2007. Two new nuclear isolation buffers for plant DNA flow cytometry: a test with 37 species. Ann. Bot. 100, 875–888. https://doi.org/10.1093/aob/mcm152.

Luo, M.C., Deal, K.R., Akhunov, E.D., Akhunova, A.R., Anderson, O.D., Anderson, J.A., Blake, N., Clegg, M.T., Coleman-Derr, D., Conley, E.J., Crossman, C.C., Dubcovsky, J., Gill, B.S., Gu, Y.Q., Hadam, J., Heo, H.Y., Huo, N., Lazo, G., Ma, Y., Matthews, D.E., McGuire, P.E., Morrell, P.L., Qualset, C.O., Renfro, J., Tabanao, D., Talbert, L.E., Tian, C., Toleno, D.M., Warburton, M.L., You, F.M., Zhang, W., Dvorak, J., 2009. Genome comparisons reveal a dominant mechanism of chromosome number reduction in grasses and accelerated genome evolution in Triticeae. PNAS 106, 15780–15785. https://doi.org/10.1073/pnas.0908195106.

Mandáková, T., Lysák, M.A., 2018. Post-polyploid diploidization and diversification through dysploid changes. Curr. Opin. Plant Biol. 42, 55–65. https://doi.org/10.1016/j.pbi.2018.03.001.

Marrero-Rodríguez, Á., Díaz-Bertrana, M., Scholz, S., 2023. *Helianthemum tibiabinae* Marrero-Rodr., Díaz-Bertrana & S. Scholz sp. nov., (Cistaceae) nueva especie para Fuerteventura. Islas Canarias. Bot. Macaronés. 32, 95–108.

Martín-Hernanz, S., Albaladejo, R.G., Lavergne, S., Rubio, E., Grall, A., Aparicio, A., 2021a. Biogeographic history and environmental niche evolution in the Palearctic genus Helianthemum (Cistaceae). Mol. Phylogenet. Evol. 163, 107238. https://doi.org/10.1016/j.ympev.2021.107238.

Martín-Hernanz, S., Albaladejo, R.G., Lavergne, S., Rubio, E., Marín-Rodulfo, M., Arroyo, J., Aparicio, A., 2023a. Strong conservatism of floral morphology during the rapid diversification of the genus Helianthemum. Am. J. Bot. 110, e16155. https://doi.org/10.1002/ajb2.16155.

Martín-Hernanz, S., Aparicio, A., Fernández-Mazuecos, M., Rubio, E., Reyes-Betancort, J. A., Santos-Guerra, A., Olangua-Corral, M., Albaladejo, R.G., 2019. Maximize resolution or minimize error? using genotyping-by-sequencing to investigate the recent diversification of Helianthemum (Cistaceae). Front. Plant Sci. 10, 1416. https://doi.org/10.3389/fpls.2019.01416.

Martín-Hernanz, S., Albaladejo, R.G., Rubio, E., Volkova, P., Miara, M.D., Ulukuş, D., Sezgin, M., Aparicio, A., 2023b. A comparative karyological study of *Helianthemum* (Cistaceae): karyotype size, karyotype symmetry and evolution of chromosome number. An. Jard. Bot. Madrid 80, e136.

Martín-Hernanz, S., Velayos, M., Albaladejo, R.G., Aparicio, A., 2021b. Systematic implications from a robust phylogenetic reconstruction of the genus *Helianthemum* (Cistaceae) based on genotyping-by-sequencing (GBS) data. An. Jard. Bot. Madrid 78, e113.

Medeiros-Neto, E., Nollet, F., Moraes, A.P., Felix, L.P., 2017. Intrachromosomal karyotype asymmetry in Orchidaceae. Genet. Mol. Biol. 40, 610–619. https://doi.org/10.1590/1678-4685-GMB-2016-0264.

Minh, B.Q., Schmidt, H.A., Chernomor, O., Schrempf, D., Woodhams, M.D., von Haeseler, A., Lanfear, R., 2020. IQ-TREE 2: new models and efficient methods for phylogenetic inference in the genomic era. Mol. Biol. Evol. 37, 1530–1534. https://doi.org/10.1093/molbev/msaa015.

Moeglein, K.M., Chatelet, D.S., Donoghue, M.J., Edwards, E.J., 2020. Evolutionary dynamics of genome size in a woody plant radiation. Am. J. Bot. 107, 1529–1541. https://doi.org/10.1002/ajb2.1544.

Moraes, A.P., Engel, T.B.J., Forni-Martins, E.R., Barros, F., Felix, L.P., Cabral, J.S., 2022. Are chromosome number and genome size associated with habit and environmental niche variables? Insights from the Neotropical orchids. Ann. Bot. 130, 11–25. https://doi.org/10.1093/aob/mcac021.

Moreno-Aguilar, M.F., Inda, L.A., Sánchez-Rodríguez, A., Arnelas, I., Catalán, P., 2022. Evolutionary dynamics of the repeatome explains contrasting differences in genome sizes and hybrid and polyploid origins of grass Loliinae lineages. Front. Plant Sci. 13, 901733. https://doi.org/10.3389/fpls.2022.901733.

Pagel, M., 1999. Inferring the historical patterns of biological evolution. Nature 401, 877–884. https://doi.org/10.1038/44766.

Paradis, E., Schliep, K., 2019. ape 5.0: an environment for modern phylogenetics and evolutionary analyses in R. Bioinformatics 35, 526–528. https://doi.org/10.1093/bioinformatics/bty633.

Paszko, B., 2006. A critical review and a new proposal of karyotype asymmetry indices. Plant Syst. Evol. 258, 39–48. https://doi.org/10.1007/s00606-006-0416-9.

Pellicer, J., Hidalgo, O., Dodsworth, S., Leitch, I.J., 2018. Genome size diversity and its impact on the evolution of land plants. Genes 9, 88. https://doi.org/10.3390/genes9020088.

Pennell, M.W., Eastman, J.M., Slater, G.J., Brown, J.W., Uyeda, J.C., FitzJohn, R.G., Alfaro, M.E., Harmon, L.J., 2014. geiger v2.0: an expanded suite of methods for fitting macroevolutionary models to phylogenetic trees. Bioinformatics 30, 2216–2218. https://doi.org/10.1093/bioinformatics/btu181.

Peruzzi, L., Eroğlu, H.E., 2013. Karyotype asymmetry: again, how to measure and what to measure? Comp. Cytogenet. 7, 1–9. https://doi.org/10.3897/CompCytogen.v7i1.4431.

Peruzzi, L., Leitch, I.J., Caparelli, K.F., 2009. Chromosome diversity and evolution in Liliaceae. Ann. Bot. 103, 459–475. https://doi.org/10.1093/aob/mcn230.

Rebolé, Á., Acevedo-Rodríguez, A., García García, A., 2021. Nueva especie del género *Helianthemum* Miller (Cistaceae) para la isla de La Palma (Islas Canarias). Vieraea 47, 65–78. https://doi.org/10.31939/vieraea.2021.47.06.

Revell, L.J., 2012. phytools: an R package for phylogenetic comparative biology (and other things). Methods Ecol. Evol. 3, 217–223. https://doi.org/10.1111/j.2041-210X.2011.00169.x.

Rice, A., Glick, L., Abadi, S., Einhorn, M., Kopelman, N.M., Salman-Minkov, A., Mayzel, J., Chay, O., Mayrose, I., 2015. The Chromosome Counts Database (CCDB) – a community resource of plant chromosome numbers. New Phytol. 206, 19–26. https://doi.org/10.1111/nph.13191.

Sader, M., Vaio, M., Cauz-Santos, L.A., Dornelas, M.C., Carneiro Vieira, M.L., Melo, O.T., Pedrosa-Harand, A., 2021. Large vs small genomes in *Passiflora*: the influence of the mobilome and the satellitome. Plant Cell Tiss. Org. Cult. 145, 53–86. https://doi.org/10.1007/s00425-021-03598-0.

Schubert, I., Lysák, M.A., 2011. Interpretation of karyotype evolution should consider chromosome structural constraints. Trends Genet. 27, 207–216. https://doi.org/10.1016/j.tig.2011.03.004.

Senderowicz, M., Nowak, T., Rojek-Jelonek, M., Bisaga, M., Papp, L., Weiss-Scheeweiss, H., Kolano, B., 2021. Descending dysploidy and bidirectional changes in genome size accompanied Crepis (Asteraceae) evolution. Genes 12, 1436. https://doi.org/10.3390/genes12091436.

Serra, L., Hernández, J.C., Alonso, M.Á., Crespo, M.B., 2023. *Helianthemum bilyanense* (Cistaceae), a new gypsum-halophytic specialist species from south-eastern Spain related to *H. polygonoides*. Plant Biosyst. 157, 939–949. https://doi.org/10.1080/11263504.2023.2231939.

Shafir, A., Halabi, K., Baumer, E., Mayrose, I., 2024. ChromEvol vol 3: modeling rate heterogeneity in chromosome number evolution. New Phytol. 245, 1787–1800. https://doi.org/10.1111/nph.20339.

Smith, S.A., O'Meara, B.C., 2012. treePL: divergence time estimation using penalized likelihood for large phylogenies. Bioinformatics 28, 2689–2690. https://doi.org/10.1093/bioinformatics/bts492.

Stebbins, G.L., 1971. Chromosomal evolution in higher plants. Edward Arnold, London, UK.

Techio, V.H., Davide, L.C., Cagliari, A., Barbosa, S., Vander Pereira, A., 2010. Karyotypic asymmetry of both wild and cultivated species of Pennisetum (Poaceae, Poales). Bragantia 69, 273–279. https://doi.org/10.1590/S0006-87052010000200003.

Tkach, N., Winterfeld, G., Röser, M., 2025. Genome sizes of grasses (Poaceae), chromosomal evolution, paleogenomics and the ancestral grass karyotype (AGK). Plant Syst. Evol. 311, 4. https://doi.org/10.1007/s00606-024-01934-x.

Veselý, P., Bureš, P., Šmarda, P., Pavlíček, T., 2012. Genome size and DNA base composition of geophytes: the mirror of phenology and ecology? Ann. Bot. 109, 65–75. https://doi.org/10.1093/aob/mcr267.

Veselý, P., Šmarda, P., Bureš, P., Stirton, C., Muasya, A.M., Mucina, L., Horová, L., Veselá, K., Šilerová, A., Šmerda, J., Knápek, O., 2020. Environmental pressures on stomatal size may drive plant genome size evolution: evidence from a natural experiment with Cape geophytes. Ann. Bot. 126, 323–330. https://doi.org/10.1093/aob/mcaa095.

Vitales, D., Álvarez, I., García, S., Hidalgo, O., Nieto Feliner, G., Pellicer, J., Vallès, J., Garnatje, T., 2020. Genome size variation at constant chromosome number is not correlated with repetitive DNA dynamism in *Anacyclus* (Asteraceae). Ann. Bot. 125, 611–623. https://doi.org/10.1093/aob/mcz183.

Wang, G., Zhou, N., Chen, Q., Yang, Y., Yang, Y., Duan, Y., 2023. Gradual genome size evolution and polyploidy in *Allium* from the Qinghai–Tibetan Plateau. Ann. Bot. 131, 109–122. https://doi.org/10.1093/aob/mcab155.

Weiss-Schneeweiss, H., Greilhuber, J., Schneeweiss, G.M., 2006. Genome size evolution in holoparasitic *Orobanche* (Orobanchaceae) and related genera. Am. J. Bot. 93, 148–156. https://doi.org/10.3732/ajb.93.1.148.

Weiss-Schneeweiss, H., Schneeweiss, G.M., 2013. Karyotype diversity and evolutionary trends in angiosperms. Genome size and the phenotype. In: Leitch, I.J., Greilhuber, J., Doležel, J., Wendel, J. (Eds.), Plant Genome Diversity 2. Springer-Verlag, Vienna, pp. 209–230.

Zhang, C., Rabiee, M., Sayyari, E., Mirarab, S., 2018. ASTRAL-III: polynomial time species tree reconstruction from partially resolved gene trees. BMC Bioinf. 19 (Suppl 6), 153. https://doi.org/10.1186/s12859-018-2129-y.

Zhang, Y., Zhou, S., Chen, Y., Zhang, P., Zhang, Y., Cai, J., Nie, Z., Zhang, L., 2025. New insights into interspecies relationships, chromosomal evolution, and hybrid identification in the *Lycoris* Herb. BMC Plant Biol. 25, 78. https://doi.org/10.1186/s12870-025-06112-w.